Critical dynamics of a dynamical version of the classical Heisenberg model

D. C. Rapaport
Physics Department, Bar-Ilan University, Ramat-Gan 52900, Israel

D. P. Landau
Center for Simulational Physics, University of Georgia, Athens, Georgia 30602
(Received 17 October 1995)

We have performed large-scale molecular dynamics simulations of a dynamical variant of the classical Heisenberg model in which the spins are replaced by interacting ''linear molecules,'' each of which has two rotational degrees of freedom. The Hamiltonian consists of rotational kinetic-energy terms as well as nearest-neighbor Heisenberg-like interactions $-J\mathbf{s}_i\cdot\mathbf{s}_j$, where $\mathbf{s}_i$ is a unit vector specifying the orientation of the molecule at lattice site i. Systems of size up to 64^3 spins on the simple cubic lattice have been studied, and thermostatting is used to maintain strictly constant temperature. We determined the dynamic structure function from the time- and space-displaced correlation functions, and found good agreement with the predictions of the dynamic scaling theory with a dynamic critical exponent of $z=1.5$. Results are compared and contrasted with data from spin-dynamics calculations on classical Heisenberg ferromagnets and antiferromagnets. [S1063-651X(96)07605-2]

PACS number(s): 64.60.Ht, 75.40.Gb, 75.10.Hk, 02.70.Ns

I. INTRODUCTION

Over several decades one of the most important methods of studying the critical behavior of interacting many-body systems has involved Monte Carlo simulation. This approach, together with exact series enumeration and methods originating from the renormalization group, has resulted in high-quality critical exponent estimates [1] for numerous models, despite the fact that analytic solutions for these models have so far proved unobtainable.

Surprisingly, the molecular dynamics (MD) approach [2,3] has, with only a single exception [4], not been applied to the study of critical phenomena. There appear to be two reasons for this situation. The first is that many of the systems studied do not have an obvious classical-mechanical formulation, principally due to the quantum origins of spin, which is the basic element of most models studied in this context. The second is the requirement for precise temperature regulation near the critical point; the most familiar form of MD is carried out at constant energy, corresponding to the microcanonical ensemble, rather than in the canonical ensemble where the critical temperature is a well-defined state point.

Neither of these reasons precludes the use of MD in the study of critical phenomena. It is possible to construct mechanical models belonging to the same universality classes as some of the better known spin systems. The resulting equations of motion can then be modified, so that instead of the system being tied to a constant-energy hypersurface in phase space (the microcanonical ensemble), the dynamics can be subjected to a constant-temperature constraint, or thermostat, which leads to the equilibrium behavior of the canonical ensemble. Although this method is often employed for simulating fluids [5,6], one example being a homogeneously sheared flow, where it is used to counteract the effects of viscous heating, we are not aware of it having been utilized previously in the study of critical phenomena.

While the static aspects of critical phenomena are relatively well understood, e.g., [7], our knowledge of the dynamical side of this problem is on a less sound footing. The stochastic nature of Monte Carlo simulation precludes its use in the study of dynamical critical behavior, with the exception of critical relaxation [8,9]. The use of MD, on the other hand, permits the modeling of the true dynamical behavior, in which propagating modes play a key role. Our goal has been to apply the constant-temperature MD technique to a system of coupled linear molecules, whose equilibrium static properties are exactly those of the classical Heisenberg ferromagnet, with a view to determining how well the predictions of dynamical scaling theory are satisfied, and how the nature of the dynamics affects the dynamical universality class. These results represent the first study of dynamical critical behavior in a system whose dynamics incorporates inertial effects; while there have been dynamical studies that preclude the role of inertia [10], there is good reason to believe that the presence of kinetic energy could have a significant impact on the critical dynamics.

The organization of this paper is as follows. In Sec. II we introduce the model, provide an overview of the dynamical scaling theory of critical phenomena as it applies to this particular study, and mention previous numerical work on related problems. In Sec. III the computational methodology is discussed. The results of the simulations, together with comparisons with theory and other numerical studies, appear in Sec. IV. Our conclusions are presented in Sec. V.

II. BACKGROUND

A. Model

In the present study, the spins of the familiar classical Heisenberg model are replaced by linear molecules—for convenience we will continue to apply the term ''spin'' to each molecule—that are free to rotate about the sites of a regular simple cubic lattice (needless to say, the same ap-

proach can also be applied to other kinds of continuous spin systems). Assuming that nearest neighbors interact via the usual Heisenberg spin-exchange interaction, the Hamiltonian for the system can be written (for zero external field)

$$\mathscr{H}=\frac{1}{2}I\sum_i \omega_i^2-J\sum J_{(i,j)}\,\mathbf{s}_i\cdot\mathbf{s}_j, \tag{1}$$

where $\mathbf{s}_i$ is the unit vector along the molecular axis (or spin direction), $\boldsymbol{\omega}_i$ the angular velocity, I the moment of inertia of the molecule, and J the strength of the spin-exchange interaction. The second of the sums is over all pairs of nearest-neighbor spins, with periodic boundaries used to reduce finite-size effects.

A straightforward derivation of the Hamilton equations [11] from (1) results in a pair of first-order equations of motion for each spin i,

$$I\dot{\boldsymbol{\omega}}_i=J\mathbf{s}_i\times\sum_j \mathbf{s}_j, \tag{2}$$

$$\dot{\mathbf{s}}_i=\boldsymbol{\omega}_i\times\mathbf{s}_i, \tag{3}$$

where the sum is over the neighbors j of spin i. Equation (2) is just the Euler equation for a linear rigid body.

B. Dynamic scaling theory

The general framework for classifying and analyzing dynamical critical phenomena is well established [12,13]. The scheme used there for assigning systems to different universality classes is based on entirely general considerations involving the underlying dynamics and applicable conservation laws. Among other results, it was demonstrated how systems with the same static critical behavior (such as ferromagnets and antiferromagnets), which therefore belonged to the same static universality class, can belong to different dynamic universality classes.

The study of critical dynamics deals with the space- and time-displaced spin-correlation function

$$C^k(\mathbf{r}-\mathbf{r}',t)=\langle s^k_{\mathbf{r}}(t)s^k_{\mathbf{r}'}(0)\rangle-\langle s^k_{\mathbf{r}}(t)\rangle\langle s^k_{\mathbf{r}'}(0)\rangle, \tag{4}$$

where $\langle\,\rangle$ denotes an ensemble average and $k=x,y,z$ are the Cartesian spin components. For the purposes of this analysis the spins are indexed by a vector $\mathbf{r}$, which also provides the spatial coordinates of the lattice sites (assuming that the lattice spacing is unity). The Fourier transform of (4) is the (real-valued) experimentally observable dynamic structure (or neutron-scattering) function

$$S^k(\mathbf{q},\omega)=\frac{1}{\sqrt{2\pi}}\sum_{\mathbf{r},\mathbf{r}'}\exp[i\mathbf{q}(\mathbf{r}-\mathbf{r}')]\int_{-\infty}^{+\infty}\exp(i\omega t)\times C^k(\mathbf{r}-\mathbf{r}',t)dt. \tag{5}$$

The assumption is now made that $S^k(\mathbf{q},\omega)$ can be expressed in terms of the correlation length ξ,

$$S^k_\xi(\mathbf{q},\omega)=\frac{1}{\omega_m(\mathbf{q},\xi)}\,S^k_\xi(\mathbf{q})f_1\left(\frac{\omega}{\omega_m(\mathbf{q},\xi)},\mathbf{q},\xi\right), \tag{6}$$

where $S^k_\xi(\mathbf{q})$ is given by

$$S^k_\xi(\mathbf{q})=\int_{-\infty}^{+\infty}S^k_\xi(\mathbf{q},\omega)d\omega, \tag{7}$$

f_1 is a normalized shape function satisfying

$$\int_{-\infty}^{+\infty}f_1(x,\mathbf{q},\xi)dx=1, \tag{8}$$

and the characteristic frequency $\omega_m(\mathbf{q},\xi)$ is defined to be the median value determined from the integral

$$\int_{-\omega_m(\mathbf{q},\xi)}^{+\omega_m(\mathbf{q},\xi)}S^k_\xi(\mathbf{q},\omega)d\omega=\frac{1}{2}\,S^k_\xi(\mathbf{q}). \tag{9}$$

The dynamic scaling hypothesis [12,13] states that in the critical region ω_m has the functional form

$$\omega_m(\mathbf{q},\xi)=q^z\Omega_1(q\xi), \tag{10}$$

where z is the dynamical critical exponent, and that the function f_1 also depends only on the product $q\xi$ (where $q=|\mathbf{q}|$), but not on the values of q and ξ separately; thus Eq. (6) becomes

$$S^k_\xi(\mathbf{q},\omega)=\omega_m^{-1}S^k_\xi(\mathbf{q})f_2(\omega/\omega_m,q\xi). \tag{11}$$

For finite-size systems, the divergent correlation length ξ is limited by the linear size of the system L, and in the spirit of finite-size scaling theory [14] we can replace ξ by L in (10) and (11) to obtain [10]

$$\omega_m(\mathbf{q},L)=L^{-z}\Omega_2(qL) \tag{12}$$

and

$$S^k_L(\mathbf{q},\omega)=\omega_m^{-1}S^k_L(\mathbf{q})f_2(\omega/\omega_m,qL). \tag{13}$$

If we now substitute (12) into (13) we obtain

$$\frac{S^k_L(\mathbf{q},\omega)}{S^k_L(\mathbf{q})}=L^z f_3(\omega L^z,qL). \tag{14}$$

The form of the arguments of the functions f_3 and Ω_2 provides a clear guide to the kinds of tests that should be carried out on the measured dynamic structure function in order to establish the applicability of dynamic scaling.

All that remains is to determine a theoretical estimate for the exponent z based on a knowledge of the low-frequency spin-wave dispersion relation at low temperatures [15]. For the Heisenberg ferromagnet, where $\omega(q)$ is quadratic in q, both dynamic scaling and renormalization group theory predict [12,13] that

$$z=3-\beta/\nu, \tag{15}$$

where β and ν are familiar static exponents whose three-dimensional (3D) values are to be found in [16], while for the antiferromagnet, where $\omega(q)$ is linear, the exponent value is

$$z=d/2, \tag{16}$$

where d is the dimensionality (these results apply for d below the upper critical dimension). In 3D these predictions correspond to $z=2.48$ for the ferromagnet and $z=1.5$ for the antiferromagnet. The reason the antiferromagnetic version of the model is introduced will become apparent in Sec. IV.

C. Previous numerical work

An alternative approach to studying $S(\mathbf{q},\omega)$ is based on equations of motion that exclude all mention of inertial effects. The Hamiltonian in this case (for zero external field) is exactly that of the classical Heisenberg model,

$$\mathscr{H}=-J\sum_{(i,j)}\mathbf{s}_i\cdot\mathbf{s}_j\,, \tag{17}$$

and the equations of motion, derived as the classical limit of the quantum mechanical equations [17], have the form

$$\dot{\mathbf{s}}_i=J\mathbf{s}_i\times\sum_j\mathbf{s}_j\,. \tag{18}$$

These equations describe spins precessing in the local fields created by their neighbors, and conserve both magnetization and interaction energy. Given that they are significantly different from those used in the MD approach—Eqs. (2) and (3)—there is little reason to expect that the dynamical properties will have very much in common.

Since there is no kinetic energy defined for this ''spin-dynamics'' model, results for a given temperature can only be obtained by first generating a set of states drawn from the canonical ensemble by some suitable Monte Carlo procedure and then using these states as the initial configurations of a series of independent dynamical computations. This approach has been used in the spin-dynamics study of the dynamical properties of Heisenberg ferromagnets [10] and antiferromagnets [18] on the bcc lattice. In both cases the measured dynamic structure function $S(\mathbf{q},\omega)$ was found to obey dynamic scaling theory, and the z exponents found to have the theoretically predicted values; finite-size effects seemed more pronounced in the antiferromagnetic case.

III. METHODOLOGY

A. Equations of motion

By redefining the time unit to be $\sqrt{I/J}$ we can eliminate the quantities I and J from the equations of motion, so that Eq. (2) becomes

$$\dot{\boldsymbol{\omega}}_i=\mathbf{s}_i\times\mathbf{g}_i\,, \tag{19}$$

where

$$\mathbf{g}_i=\sum_j\mathbf{s}_j \tag{20}$$

is a sum over the nearest neighbors of i. For computational convenience the pair of first-order Eqs. (3) and (19) can be replaced by a single second-order equation [3]

$$\ddot{\mathbf{s}}_i=\mathbf{g}_i-(\mathbf{s}_i\cdot\mathbf{g}_i+\dot{\mathbf{s}}_i^2)\mathbf{s}_i\,. \tag{21}$$

The derivation of this equation assumes $\boldsymbol{\omega}_i\cdot\mathbf{s}_i=0$, but if this condition is incorporated into the construction of the initial state then it is clear from the form of the first-order equations that it always remains true; note that $\boldsymbol{\omega}_i$ itself does not appear in (21).

The equations of motion (21) are energy conserving. Study of the critical region requires a more precisely regulated temperature than that obtainable from MD of this kind, which is subject to considerable (size-dependent) temperature fluctuations. The solution to this problem is the introduction of a thermostat. To convert the equations of motion into a form that conserves kinetic energy, and thus temperature, the standard procedure of introducing a Lagrange multiplier is followed. The result [3] is that the equation of motion (21) is replaced by

$$\ddot{\mathbf{s}}_i=\mathbf{g}_i-(\mathbf{s}_i\cdot\mathbf{g}_i+\dot{\mathbf{s}}_i^2)\mathbf{s}_i+\alpha\dot{\mathbf{s}}_i\,, \tag{22}$$

where

$$\alpha=-\frac{\sum_m\dot{\mathbf{s}}_m\cdot[\mathbf{g}_m-(\mathbf{s}_m\cdot\mathbf{g}_m+\dot{\mathbf{s}}_m^2)\mathbf{s}_m]}{\sum_m\dot{\mathbf{s}}_m^2} \tag{23}$$

is the Lagrange multiplier that ensures constant kinetic energy; α is evaluated at each time step, immediately following the interaction calculation, and used in the right-hand side of (22). The phase-space trajectories no longer obey Newtonian dynamics, but the deviations are small (obviously decreasing as the system size is increased); the equilibrium configurational properties are now precisely those of the canonical ensemble [5,6].

The equations of motion (22) are solved using a standard fourth-order predictor-corrector method [2,3], with a time step $\Delta t=0.01$. To reduce the cumulative effects of numerical inaccuracy the lengths of the vectors $\mathbf{s}_i$ are renormalized every 50 time steps. Minor temperature adjustments (since there are two degrees of freedom per spin $T=\langle\dot{\mathbf{s}}_i^2\rangle$ in units where both I and the Boltzmann constant k_B are unity) are made by rescaling the values of $\dot{\mathbf{s}}_i$ every 200 steps; without this, a temperature drift of one part in 10^{-3} occurs over 10^6 time steps, an amount which, though small, begins to approach the temperature precision required for critical-point studies.

The results reported here involve simple cubic lattices of size $N=L^3$ spins, with L ranging from 16 to 64. The complete run lengths are approximately 2.2×10^6 time steps in each case, of which the first 3×10^5 are used to allow the system to equilibrate. The initial state consists of all spins parallel, with angular velocities having a fixed magnitude based on the desired temperature and randomly assigned directions satisfying the requirement $\boldsymbol{\omega}_i\cdot\mathbf{s}_i=0$. Typical computational speed for the largest system is approximately 4 μs per spin step on an IBM 6000/590 processor; thus the largest run reported here requires roughly 700 hours of computation.

It should be pointed out that this approach can be used not only to study the dynamical behavior of the model—the subject of this paper—but also the equilibrium static properties; this will be addressed elsewhere. Although MD appears to be competitive with the basic metropolis Monte Carlo approach, it is unable to compete with recent refinements of the method (such as cluster sampling and histogram reweighting) that

are able to yield extremely precise estimates of the static critical properties [16]. But, unlike Monte Carlo simulation, MD provides the means for studying critical spin dynamics: the only form of spin ''dynamics'' that can be studied by Monte Carlo is entirely stochastic in nature, whereas MD correctly accounts for the contribution of inertial effects to the dynamics.

B. Spin correlations

In studying the spin correlations we restrict the **q** vectors to those directed along the coordinate axes; this permits a considerable reduction in the computational effort and storage requirements of the program (already close to 60 Mbytes for the largest system) without any reduction in the effectiveness of the analysis. If, for example, we choose $\mathbf{q}=(q,0,0)$, where the values of q are limited by the periodic boundaries to $q=2\pi n/L$ $(n=1,2,\ldots)$, the spatial Fourier transform in (5) becomes

$$\sum_{\mathbf{r},\mathbf{r}'} \exp[i\mathbf{q}\cdot(\mathbf{r}-\mathbf{r}')]s^k_{\mathbf{r}}(t)s^k_{\mathbf{r}'}(0)=\sum_{r_x r'_x} \exp[iq(r_x-r'_x)] \times\left[\sum_{r_y,r_z} s^k_{\mathbf{r}}(t)\right]\left[\sum_{r'_y,r'_z} s^k_{\mathbf{r}'}(0)\right]. \tag{24}$$

This implies that only a 1D Fourier transform of the correlations between the summed spin components in the $y-z$ plane is required, rather than a full 3D transform involving all the spins; a minor disadvantage of the technique (not relevant to the present study) is that the original spatial correlations cannot be recovered from these results. For improved statistics, the other on-axis components of **q** can be similarly treated, and the three sets of results averaged.

For a finite system at T_c the magnetization (per spin)

$$\mathbf{m}=\frac{1}{N}\sum_i \mathbf{s}_i \tag{25}$$

is nonzero, so the spin correlations should be decomposed into longitudinal (parallel to **m**) and transverse parts, just as is the practice below T_c. Thus instead of evaluating the correlations between the Cartesian components of the spin vectors, we consider the correlations between the spin components,

$$\mathbf{s}^l_i=(\mathbf{s}_i\cdot\mathbf{e}_m)\mathbf{e}_m, \tag{26}$$

$$\mathbf{s}^t_i=\mathbf{s}_i-\mathbf{s}^l_i, \tag{27}$$

where $\mathbf{e}_m=\mathbf{m}/|\mathbf{m}|$. This leads us to the longitudinal and transverse dynamic structure functions $S^l(\mathbf{q},\omega)$ and $S^t(\mathbf{q},\omega)$, the latter computed as an average of separate contributions from each of the three components of $\mathbf{s}^t_i$.

The spin correlations are measured every 20 time steps; a full set of correlation function measurements extends over an interval exceeding 400 time units (providing a total of 2049 data points) for $L=16$, 32, 48, and twice this value for $L=64$. To improve the statistics, the measurement intervals are made to overlap; collection of data for a new set of correlation measurements is begun every 128th measurement—this implies that there are 16 sets of measurements in progress simultaneously for the three smaller systems, and 32 for the largest. A total of 600 such intervals contribute to the final result; in order to estimate error bar magnitudes the results are divided into six sets and the rms spread used as a measure of the statistical error.

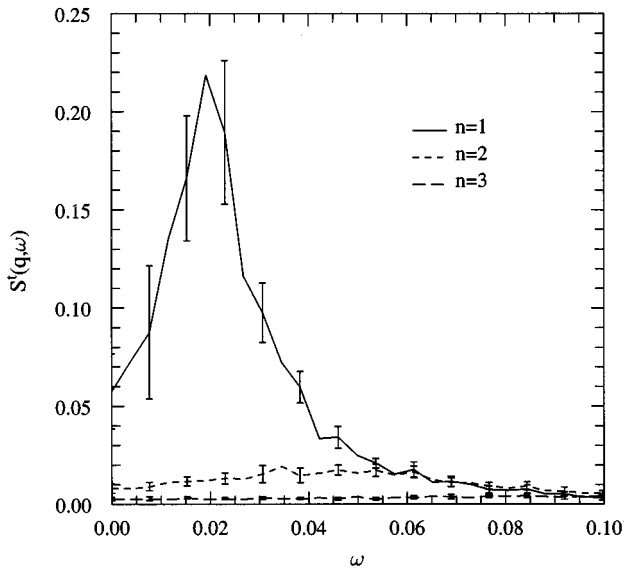

FIG. 1. Transverse dynamic structure function for $L=64$ and $q=n\pi/32$, $n=1,\ldots,3$; typical error bars are shown.

IV. RESULTS

In this discussion the focus is on the dynamical behavior resulting from MD simulations at the critical temperature T_c of the infinite system. The Monte Carlo method has proved capable of producing very precise T_c estimates, as well as critical exponent values; for the simple cubic lattice (in units of J) $T_c=1.443$ (the actual value is $1.442\,929\pm0.000\,077$) [16].

In Fig. 1 we show the transverse dynamic structure function $S^t(q,\omega)$ for the largest system ($L=64$) and for the lowest three q values, namely, $q=n\pi/32$, $n=1,\ldots,3$ (here and in subsequent figures error bars are included for a fraction of the data points only). The MD results show spin-wave peaks at q-dependent frequencies (note that q and ω are expressed in dimensionless MD units). There is no evidence for a central peak (corresponding to spin diffusion) in these results; if one exists it is completely swamped by the pair of spin-wave peaks (the curve is of course symmetric about $\omega=0$). Corresponding results for the longitudinal function $S^l(q,\omega)$ are shown in Fig. 2; here the central peak is the only feature present. By way of contrast, the spin-dynamics approach (on the bcc lattice) shows evidence of a central peak, even in the transverse case, for both the ferromagnetic [10] and antiferromagnetic [18] systems.

The $S(q,\omega)$ results presented here have not been subjected to any smoothing, and because the correlation functions are measured out to sufficiently long times that, despite critical slowing down, the observable correlations are essentially at the noise level [roughly 0.01 for the transverse correlation functions that have been normalized so that

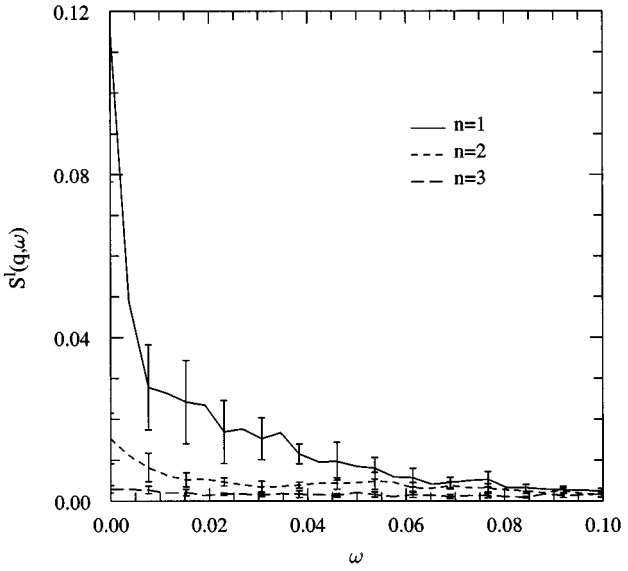

FIG. 2. Longitudinal dynamic structure function (see Fig. 1).

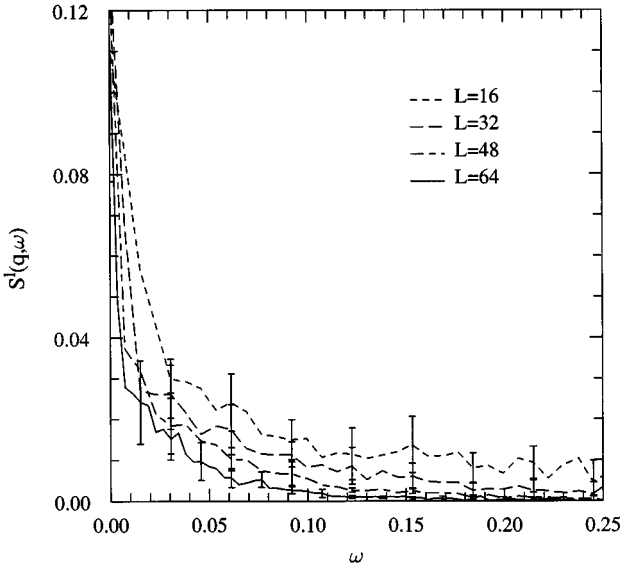

FIG. 4. Longitudinal dynamic structure function (see Fig. 3).

$C^t(\mathbf{r},0)=1$], there is no need to apply a window function [19] to the data prior to the Fourier transformation, as was the case in the spin-dynamics study of the ferromagnet [10]. While windowing does eliminate much of the noise from the data, it also has the effect of lowering and broadening any peaks that are present; even a Gaussian window function that drops to about 0.04 of the maximum height at the extreme of the $L=64$ measurement interval reduces the $S^t(q,\omega)$ peak height by about 10%, and this is best avoided.

To provide some indication of the way the peaks change as the system size increases, Figs. 3 and 4 show $S^t(q,\omega)$ and $S^l(q,\omega)$ at the smallest possible wave number $q=2\pi/L$ for $L=16,...,64$. The peaks are seen to become narrower as L increases, and in the transverse case, to increase in height and also shift to smaller ω.

The dynamic scaling theory makes a specific prediction, given by Eq. (12), as to the way the median frequency should vary with q and L, namely, that for the correct choice of exponent z, the value of $L^z\omega_m$ should depend only on the product qL. In Fig. 5 we show these results for $qL/2\pi=1,\ldots,4$ using the antiferromagnetic exponent value $z=1.5$. Note the practically horizontal line for $n=1$, as predicted by dynamic scaling theory; a small change in the value of z (by a few percent) destroys this theoretically predicted behavior. The quality of the results drops for higher n because shorter wavelengths are involved.

The other prediction of dynamic scaling theory to be tested here is the nature of the scaled form of $S^t(q,\omega)$, namely, Eq. (14). Figure 6 shows the results for $qL/2\pi=1,2$

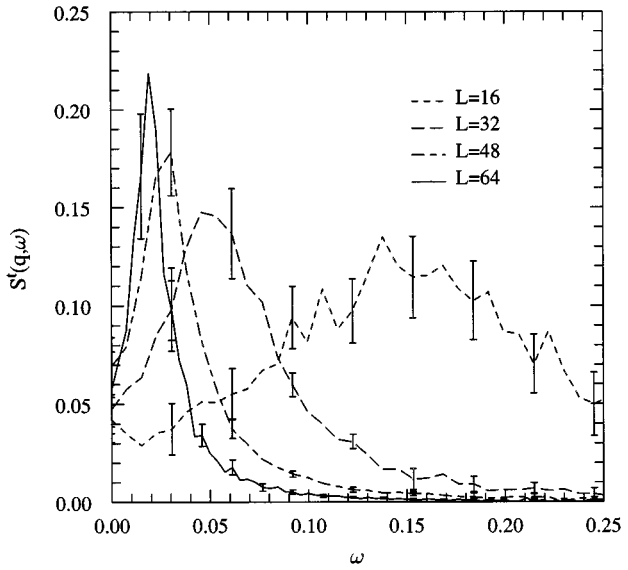

FIG. 3. Transverse dynamic structure function for $q=2\pi/L$ and $L=16,32,48,64$.

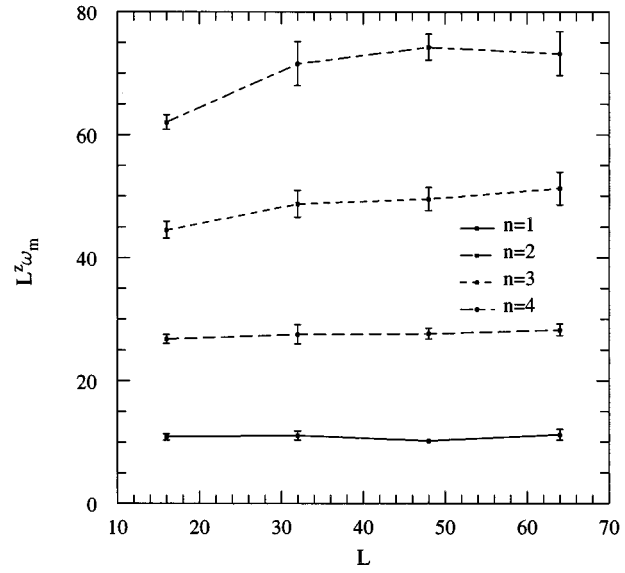

FIG. 5. Scaled median frequency $L^z\omega_m$ as a function of L for $n\equiv qL/2\pi=1,\ldots,4$.

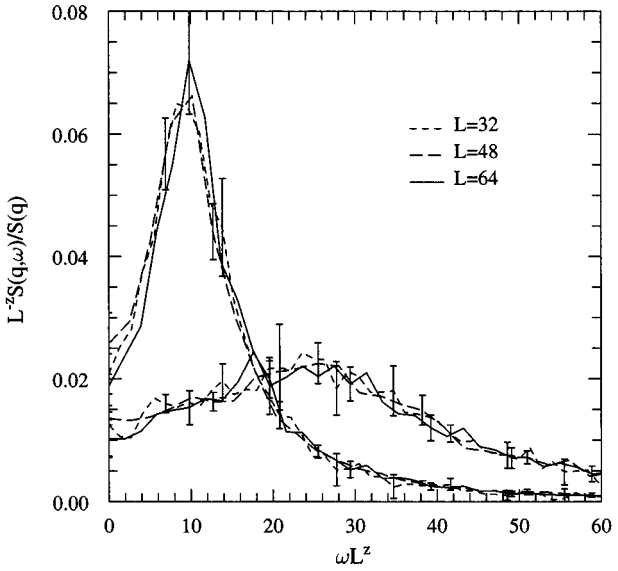

FIG. 6. Scaled transverse dynamic structure functions for $L=32,48,64$ and $qL/2\pi=1$ (left peaks) and 2 (right peaks); here $z=1.5$.

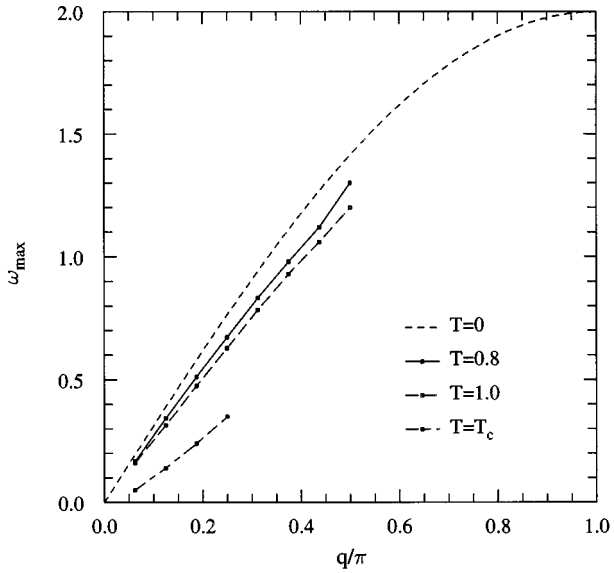

FIG. 7. Dispersion curves at and below below T_c for $L=32$; the $T=0$ result is also shown.

and $L=32,48,64$, with the exponent value $z=1.5$: as predicted, the curves for different L but the same qL coincide to within measurement accuracy (this conclusion is not particularly sensitive to a small variation—less than 10%—in z). The spread of values between the different curves is similar to that observed in the spin-dynamics study of the antiferromagnet [18].

Clearly the results are consistent with the value $z=1.5$, which is the result predicted for the antiferromagnetic Heisenberg model. The reasons for not expecting to obtain the ferromagnetic value ($z=2.48$) are that, unlike spin dynamics, the magnetization is not conserved by the MD equations of motion, and that the spin-wave dispersion relation is linear—as shown in Fig. 7 where the locations of the maxima of $S^t(q,\omega)$ are plotted for $L=32$ and temperatures 0.8, 1.0, and T_c (the $T=0$ result, $\omega(q)=2\sin(q/2)$, is also included)—the dependence exhibited by the antiferromagnet. By way of contrast, the corresponding Monte Carlo estimate for the Heisenberg ferromagnet is $z=1.96$ [20], a result due entirely to the underlying relaxation mechanism.

To emphasize the difference in the dynamics between MD and spin dynamics, Fig. 8 shows the magnetization m ($=|\mathbf{m}|$) as a function of time for the duration of the $L=64$ run; each data point is the average of the magnitude of the magnetization vector $\mathbf{m}$ over 2×10^4 time steps, an interval considerably greater than that for which individual spin correlations persist. The results appear very noisy, with no obvious correlations. In the calculation for a ferromagnet based on spin dynamics, the magnetization would remain fixed at the value reached during the preceding Monte Carlo phase.

Figure 9 shows a simple visual fit of $S(q,\omega)$ for the lowest q value ($\pi/32$) using a double Lorentzian

$$\frac{A\Gamma}{\Gamma^2+(\omega-\omega_s)^2}+\frac{A\Gamma}{\Gamma^2(\omega+\omega_s)^2} \tag{28}$$

to describe the spin-wave peaks; the parameter values are $A=2\times10^{-3}$, $\Gamma=0.01$, and $\omega_s=0.02$. The fit is of reasonable quality, although slightly too large at low ω; the quality of the data and possible residual finite-size effects do not warrant a more refined attempt at curve fitting that would include a small contribution from another Lorentzian at $\omega=0$. A somewhat poorer fit is obtained using the alternative functional form

$$\frac{A\Gamma}{\Gamma^2+(\omega^2-\omega_s^2)^2} \tag{29}$$

proposed in [12]; the values of A and Γ used here are 1.25×10^{-4} and 6×10^{-4}, respectively.

Both MD and spin dynamics support dynamic scaling, although the results differ in detail—in particular, the

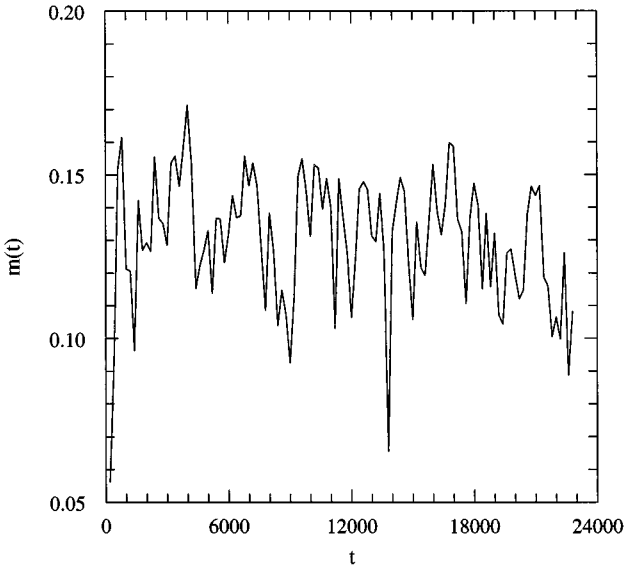

FIG. 8. Magnetization as a function of time ($L=64$).

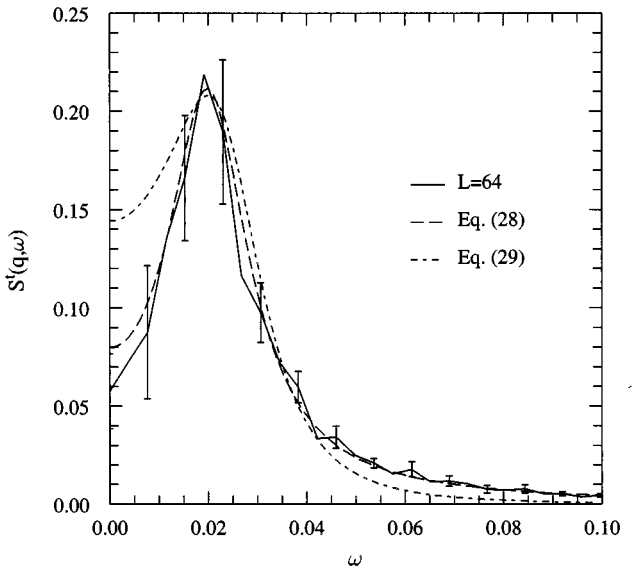

FIG. 9. Visual curve fits to $S^t(q,\omega)$ for $q=\pi/32$ ($L=64$) using the double Lorentzian of Eq. (28) and the alternative form given in Eq. (29).

strength of the transverse central peak. Because of the different dynamics, MD requires more computation than spin dynamics and does not benefit from the decorrelating effects produced by the Monte Carlo construction of initial states; furthermore, the time intervals over which the correlations are measured are several times longer for MD than for spin dynamics (in the reduced units appropriate to each problem). On the other hand, the MD approach addresses a Hamiltonian system into which other features, such as lattice vibrations, can readily be incorporated, and it also provides the basis for the study of related phenomena, such as the rotational phases of molecular crystals.

V. CONCLUSIONS

The dynamical critical behavior of a dynamical version of the Heisenberg ferromagnet has been studied by MD simulation. The results for the dynamic structure function are found to be in reasonable agreement with the predictions of dynamical scaling theory. The dynamical critical exponent z does not have the ferromagnetic value ($z=2.48$) but rather the value predicted for the antiferromagnet ($z=1.5$), indicating that the model belongs to the dynamical universality class of the antiferromagnet. The plausibility of this result derives from the fact that, due to the inclusion of the kinetic-energy term, the low-temperature dispersion relation is linear—as in the antiferromagnet—as opposed to the quadratic dependence which arises if the ferromagnetic Hamiltonian contains the potential energy term alone. The fact that the MD results differ from those obtained by the spin-dynamics approach (where the kinetic energy term is absent) is further evidence of the important role played by the equations of motion in determining the dynamical universality class.

ACKNOWLEDGMENTS

This research was supported in part by U.S.-Israel Binational Science Foundation Grant No. 92-251 and by NSF Grant No. DMR-9405018.

[1] For a review of the status of different numerical results, see D. P. Landau, Physica A **205**, 41 (1994), and references therein.
[2] M. P. Allen and D. J. Tildesley, *Computer Simulation of Liquids* (Oxford University Press, Oxford, 1987).
[3] D. C. Rapaport, *The Art of Molecular Dynamics Simulation* (Cambridge University Press, Cambridge, 1995).
[4] T. Schneider and E. Stoll, Phys. Rev. B **13**, 1216 (1976).
[5] D. J. Evans, W. G. Hoover, B. H. Failor, B. Moran, and A. J. C. Ladd, Phys. Rev. A **28**, 1016 (1983).
[6] D. J. Evans and G. P. Morriss, *Statistical Mechanics of Nonequilibrium Liquids* (Academic, London, 1990).
[7] S.-K. Ma, *Modern Theory of Critical Phenomena* (Benjamin Cummings, Reading, MA, 1976).
[8] D. P. Landau, S. Y. Tang, and S. Wansleben, J. Phys. (Paris) Colloq. **49**, 8, 1525 (1989).
[9] N. Ito, Physica A **196**, 591 (1993).
[10] K. Chen and D. P. Landau, Phys. Rev. B **49**, 3266 (1994).
[11] H. Goldstein, *Classical Mechanics*, 2nd ed. (Addison-Wesley, Reading, MA, 1980).
[12] B. I. Halperin and P. C. Hohenberg, Phys. Rev. **177**, 700 (1969).
[13] P. C. Hohenberg and B. I. Halperin, Rev. Mod. Phys. **49**, 435 (1977).
[14] *Finite-Size Scaling and Numerical Simulation of Statistical Systems*, edited by V. Privman (World Scientific, Singapore, 1990).
[15] J. M. Ziman, *Principles of the Theory of Solids*, 2nd ed. (Cambridge University Press, Cambridge, 1972).
[16] K. Chen, A. M. Ferrenberg, and D. P. Landau, Phys. Rev. B **48**, 3249 (1993).
[17] R. E. Watson, M. Blume, and G. H. Vineyard, Phys. Rev. **181**, 811 (1969).
[18] A. Bunker, K. Chen, and D. P. Landau (unpublished).
[19] W. H. Press, S. A. Teukolsky, W. T. Vetterling, and B. R. Flannery, *Numerical Recipes in C: The Art of Scientific Computing*, 2nd ed. (Cambridge University Press, Cambridge, 1992).
[20] P. Peczak and D. P. Landau, Phys. Rev. B **47**, 14 260 (1993).